Journal of Hazardous Materials 172 (2009) 675–684

Contents lists available at ScienceDirect

Journal of Hazardous Materials

journal homepage: www.elsevier.com/locate/jhazmat

Photolytic destruction of endocrine disruptor atrazine in aqueous solution under UV irradiation: Products and pathways

Cheng Chen[a], Shaogui Yang[a,*], Yaping Guo[b], Cheng Sun[a,*], Chenggang Gu[a], Bin Xu[c]

[a] State Key Laboratory of Pollution Control and Resource Reuse, School of the Environment, Nanjing University, Nanjing 210093, PR China
[b] College of Biological and Environmental Engineering, Zhejiang University of Technology, Hangzhou 310032, PR China
[c] School of Environmental Science and Engineering, State Key Laboratory of Pollution Control and Resources Reuse, Tongji University, Shanghai, PR China

ARTICLE INFO

Article history:
Received 10 April 2009
Received in revised form 14 July 2009
Accepted 14 July 2009
Available online 22 July 2009

Keywords:
Atrazine
Photolytic degradation
Pathways
Ultraviolet light

ABSTRACT

The ultraviolet (UV) photolysis of atrazine in aqueous solution was investigated at wavelength of 254 nm in this study. This paper was mainly focused on the identification of atrazine degradation intermediates by HPLC–MS/MS and its degradation mechanisms. The photodegradation products included the following seven classes: dechloro-hydroxylated products, chloro-dealkylated products, dechloro-dealkylated products, alkylic-oxidated products, delamination-hydroxylated products, olefinic products, and dechloro-hydrogenated products which were never reported in direct photolytic process, 4-isopropylamino-6-ethylamino-s-triazine (IEST), 4,6-dihydroxy-s-triazine (OOST). The main degradation products were 2-hydroxy-4-acetamido-6-ethylamino-s-triazine (OIET), 2-chloro-4-isopropyl-amino-6-methylamino-s-triazine (CIMT), 2-chloro-4,6-divinylamino-s-triazine (CVVT), 2-chloro-4-ethylamino-6-amino-s-triazine(CEAT), 2-methoxy-4-isopropyl-amino-6-methylamino-s-triazine (OIMT), 2-hydroxy-4-acetamindo-6-ethylamino-s-triazine (ODET), etc. Finally, the possible degradation mechanism was also proposed here.

1. Introduction

Atrazine (6-chloro-*N*-ethyl-*N*-(1-methylethyl)-1,3,5-triazine-2,4-diamine), one of the most widely used herbicides, has been widely applied in agricultural and forestry fields. Due to its relatively high aqueous solubility and high mobility, atrazine can be transported to groundwater by infiltration or to surface waters by water runoff, thus enter aquatic environment easily [1], therefore, it is more frequently detected in groundwater and surface water than any other herbicides in many countries [2]. Atrazine was categorized as a "possible human carcinogen" in the 1980s. Recently, as a putative endocrine disruptor, its toxic effects have been extensively studied both in experimental animals and humans [3]. Hayes et al. [4,5] found that at extremely low concentrations, atrazine could feminize amphibians and also disrupt the estrous cycle in various laboratory rat strains [6]. Besides, atrazine is also reportedly associated with decreased semen quality and fertility in men living in agricultural areas [7]. So progressively more severe limits have been imposed in recent years to its use. European countries have banned its use now and promulgated a 1.0 $\mu g\,L^{-1}$ maximum contaminant level (MCL) in drinking water for it, and the United States Environmental Protection Agency (USEPA) also set the drinking water limit at 3 $\mu g\,L^{-1}$.

Photodegradation is one of the key attenuation processes of atrazine in the environment. Numerous studies on photodegradation of atrazine have been carried out so far. It has been well documented that ultraviolet light would produce fast degradation and overall detoxification, as related to the very efficient dechlorination-hydroxylation followed dealkylation process at a slow rate [8,9]. Hequet et al.'s report [10] confirmed that chloro-dealkylateion was a secondary pathway under a medium pressure mercury source (UV–vis irradiation). Furthermore, Torrents et al. [11] suggested that during a 60-h period, 23% atrazine conversion gave rise to 14% 2-hydroxy-4-acetamido-6-ethylamino-s-triazine (OIET) and cyanuric acid, 9% chloro-dealkylated (2-chloro-4-ethylamino-6-amino-s-triazine, 2-chloro-4-isopropylamino-6-amino-s-triazine) and chloro-alkyloxidized (2-chloro-4-acetamindo-6-isopropylamino-s-triazine, and 2-hydroxy-4-acetamindo-6-ethylamino-s-triazine) products were detected, but no dechloro-dealkylated products were found. In addition, our previous report [2] proposed the four possible degradation pathways of atrazine in microwave-assisted photolytic process, namely, dealkylation, dechlorination-hydroxylation, alkylic-oxidation, and delamination-hydroxylation. It is well known that the complete mineralization of atrazine could not occurred in photolysis due to the stability of the s-triazine ring toward oxidation and its possibly final degradation

* Corresponding authors. Tel.: +86 25 83593239; fax: +86 25 83593239.
E-mail addresses: yangdlut@126.com (S. Yang), envidean@nju.edu.cn (C. Sun).

0304-3894/$ – see front matter.
doi:10.1016/j.jhazmat.2009.07.050

product was cyanuric acid (2,4,6-trihydroxy-1,3,5-triazine, CA) with a low toxicity [12,13]. Therefore, the photolytic degradation of atrazine under UV irradiation was a very complicated process, and it might follow several reaction pathways including chloro-dealkylation, dechlorination, dechloro-dealkylation, alkylic-oxidation, delamination-hydroxylation and olefination, etc. Moreover, theoretically speaking, intense UV radiation could induce direct cleavage of C–Cl bond to form dechloro-hydrogenated products, which might be another possible pathway of photolysis of atrazine. However, to the best of our knowledge, up to now, few paper systematically reported the direct photolytic products of atrazine and its degradation pathways based on 254 nm ultraviolet irradiation. Thus, our present work made an overall survey on the phototransform of atrazine under 254 nm UV irradiation, focused on more comprehensive investigation on its photolytic degradation products and mechanism.

2. Experimental

2.1. Materials

Standard atrazine (97.4% purity) was purchased from Sigma–Aldrich, dichloromethane and methanol with HPLC grade solvents were purchased from Tedia (Fairfield, OH, USA). The ultra-pure water was obtained by a Milli-Q water ion-exchange system (Millipore Co).

2.2. Methods

2.2.1. General procedure for photolytic experiments

Photolysis experiments were carried out in a 250 mL glass cylindrical reactor shown in Fig. 1, which equipped with an immersible low-pressure mercury lamp (8 W) with the prominent emission band at 254 nm, cooperated with a magnetic stir. The ultraviolet intensity was about 0.96 mW cm^{-2}.

The atrazine stock solution was prepared in methanol, less than 1% (v/v). The initial concentration of atrazine was 10 mg L^{-1} in the experiment.

2.2.2. HPLC analysis of atrazine

The HPLC (Agilent 1200, USA) analysis was carried out using a C18 column (Gemini 5 μm, 150 mm × 4.6 mm, Phenomenex), and methanol–H_2O (55:45, v/v) as mobile phase with a flow rate of 1.0 mL min^{-1}. The detection wavelength was 223 nm.

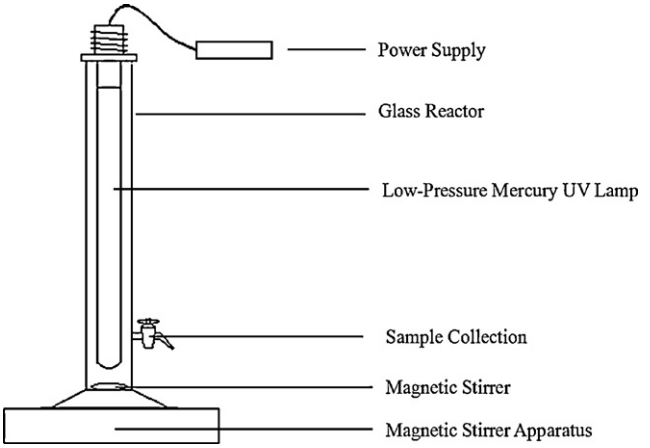

Fig. 1. Photochemical reactor.

2.2.3. Collection and HPLC and LC–MS/MS analysis of degradation products

The Supelclean ENVITM-18 solid phase extraction (SPE) tubes (Supelco, Bellefonte, PA, USA) were chosen for the enrichment of degradation products of atrazine. The SPE tubes were packed with 1 mg of silica gel bonded reversed phase parkings with average particle size at 56.0 μm. Before using, the SPE tubes were preconditioned with 10 mL of methanol, then 10 mL of distilled water and finally stored at distilled water. The reaction solutions were enriched through the SPE tubes with a flow rate of 5 mL min^{-1} under vacuum pump. The SPE tubes enriched degradation products were eluted by 5 mL methanol twice at 1 mL min^{-1} and then the eluent was dried by adding anhydrous sodium sulfate and evaporated in an evaporator, then in a gentle stream of nitrogen until the volume was less than 1.5 mL [2].

For the investigation of AT degradation, aliquots sample were collected from different reaction times and analyzed by HPLC and LC–MS/MS (Thermo LCQ Advantages QuestLCQ Duo, USA). The same LC conditions were described in Section 2.2.2 except the detection wavelengths were 223, 215, 235 nm [11,14]. The intermediates were detected by LC–MS and LC–MS/MS (Thermo, USA) equipped with atmospheric pressure chemical ionization interface (APCI) and electrospray ionization mass spectrometry (ESI-MS). The flow rate was 0.4 (APCI) or 0.2 (ESI) mL min^{-1} under isocratic conditions of methanol–water (v/v): 70:30 (APCI) or 80:20 (ESI). The capillary temperature was set at 150 °C with a voltage of 30 V for APCI and 300 °C for ESI. The spectra were acquired in the positive scan mode, over the m/z range 50–300 at 1.0 scan s^{-1}. The discharge

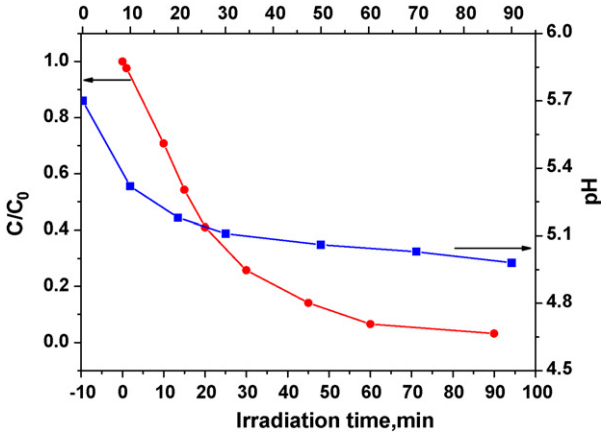

Fig. 2. Change of concentration of atrazine and solution pH vs. irradiation time.

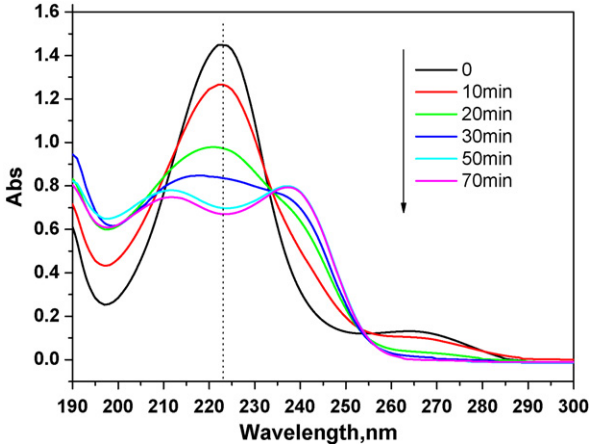

Fig. 3. UV–vis spectra of atrazine and its products in aqueous solutions.

Table 1
Structures, retention time and abbreviation of atrazine and degradation products (data without specification were obtained by HPLC/APCI–MS/MS with a isocratic condition of methanol–water (v/v): 70:30.)

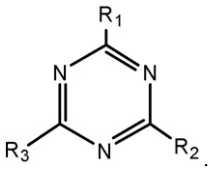

M or M + H+	Retention time (min)	APCI or ESI-MS/MS spectrum ions	Abbreviation	Compounds	R1	R2	R3
216	9.96	174	AT	2-Chloro-4-ethylamino-6-isopropylamino-s-triazine	Cl	NHC_2H_5	$NHCH(CH_3)_2$
A							
198	4.79	156,198	OIET	2-Hydroxy-4-acetamido-6-ethylamino-s-triazine	OH	NHC_2H_5	$NHCH(CH_3)_2$
B							
128	8.41	85,58	OAAT	2-Hydroxy-4,6-diamino-s-triazine (ammeline)	OH	NH_2	NH_2
156	4.72	86,114	OEAT	2-Hydroxy-4-ethylamino-6-amino-s-triazine	OH	NHC_2H_5	NH_2
170	3.76	128,170	OIAT	2-Hydroxy-4-isopropylamino-6-amino-s-triazine	OH	NH_2	$NHCH(CH_3)_2$
184	4.15	114	OIMT	2-Methoxy-4-methylamino-6-isopropylamino-s-triazine	OH	$NHCH_3$	$NHCH(CH_3)_2$
C							
147	5.98	96	COAT	2-Chloro-4-hydroxy-6-amino-s-triazine	Cl	OH	NH_2
174	6.24	89,132,159	CEAT	2-Chloro-4-ethylamino-6-amino-s-triazine	Cl	NHC_2H_5	NH_2
188	6.97	146	CIAT	2-Chloro-4-isopropylamino-6-amino-s-triazine	Cl	NH_2	$NHCH(CH_3)_2$
202	7.87	124,132,174	CIMT	2-Chloro-4-isopropylamino-6-methylamino-s-triazine	Cl	$NHCH_3$	$NHCH(CH_3)_2$
D							
157	4.61	86,139,114	OOET	2,6-Dihydroxy-4-ethylamino-s-triazine	OH	NHC_2H_5	OH
171	8.31	129	OOIT	2,4-Dihydroxy-6-isopropylamino-s-triazine	OH	$NHCOCH_3$	OH
171	5.54	129	OODT	2,4-Dihydroxy-6-acetamindo-s-triazine	OH	$NHCH(CH_3)_2$	OH
E							
170	4.80	128,170	ODAT	2-Hydroxy-4-acetamindo-6-amino-s-triazine	OH	NH_2	$NHCOCH_3$
188	6.02	146	CDAT	2-Chloro-4-acetamindo-6-amino-s-triazine	Cl	$NHCOCH_3$	NH_2
198	4.03	156,198	ODET	2-Hydroxy-4-acetamindo-6-ethylamino-s-triazine	OH	$NHCOCH_3$	NHC_2H_5
212	4.92	170,212	ODIT	2-Hydroxy-4-acetamindo-6-isopropylamino-s-triazine	OH	$NHCOCH_3$	$NHCH(CH_3)_2$
212	5.32	128,170,212	ODDT	2-Hydroxy-4,6-diacetamindo-s-triazine	OH	$NHCOCH_3$	$NHCOCH_3$
220(ESI)	12.88	175,206	COOEMT	2-Chloro-4-(2,2-dihydroxy-ethylamino)-6-methylamino-s-triazine	Cl	$NHCH_3$	$NHC(OH)_2CH_3$
228	5.42	196	ODOIT	2-Chloro-4-acetamindo-6-(2-hydroxy-isopropylamino)-s-triazine	OH	$NHCOCH_3$	$NHC(OH)(CH_3)_2$
230	12.86	188,146	CDIT	2-Chloro-4-acetamindo-6-isopropylamino-s-triazine	Cl	$NHCOCH_3$	$NHCH(CH_3)_2$
230	19.35	214,215	CDDT	2-Chloro-4,6-diacetamindo-s-triazine	Cl	$NHCOCH_3$	$NHCOCH_3$
232	8.62	190,204	COEIT	2-Chloro-4-(2-hydroxy-ethylamino)-6-isopropylamino-s-triazine	Cl	$NHCH(OH)CH_3$	$NHCH(CH_3)_2$
248	2.64	205,217,235	COIOET	2-Chloro-4-(2-hydroxy-ethylamino)-6-(2-hydroxy-isopropylamino)-s-triazine	Cl	$NHCH(OH)CH_3$	$NHC(OH)(CH_3)_2$
F							
154	4.95	112	OVAT	2-Hydroxy-4-vinylamino-6-amino-s-triazine	OH	$NHCH{=}CH_2$	NH_2
155	4.70	113,98	OOVT	2,6-Dihydroxy-4-vinylamin-s-triazine	OH	$NHCH{=}CH_2$	OH
182	5.66	154	OVET	2-Hydroxy-4-vinylamino-6-ethylamino-s-triazine	OH	$NHCH{=}CH_2$	NHC_2H_5
196	4.98	154,112,126	OIVT	2-Hydroxy-4-isopropylamino-6-vinylamino-s-triazine	OH	$NHCH{=}CH_2$	$NHCH(CH_3)_2$
198	8.57	113,127,156	CVVT	2-Chloro-4,6-divinylamino-s-triazine	Cl	$NHCH{=}CH_2$	$NHCH{=}CH_2$
G							
113	8.15	71,96	OOST	4,6-Dihydroxy-s-triazine	H	OH	OH
139	2.66	69,97,86,125	EAST	4-Ethylamino-6-amino-s-triazine	H	NHC_2H_5	NH_2
154	8.50	111	IAST	4-Isopropylamino-6-amino-s-triazine	H	NH_2	$NHCH(CH_3)_2$
166	6.86 (methanol: water = 75:25)	123	VEST	4-Vinylamino-6-ethylamino-s-triazine	H	$NHCH{=}CH_2$	NHC_2H_5
182	6.74	140	EIST	4-Ethylamino-6-isopropylamino-s-triazine	H	NHC_2H_5	$NHCH(CH_3)_2$
184	6.68	113,142,156, 184	OEEST	4-(2-Hydroxy-ethylamino)-6-ethylamino-s-triazine	H	$NHCH(OH)CH_3$	NHC_2H_5
H							
156	5.62	127,110	M-OMAT	2-Methoxy-4-methylamino-6-amino-s-triazine	OCH_3	$NHCH_3$	NH_2
169	6.50	127	M-OOVT	2-Methoxy-4-vinylamino-6-hydroxy-s-triazine	OCH_3	$NHCH{=}CH_2$	OH
170	8.96	114,142	M-OIET	2-Methoxy-4-isopropylamino-6-ethylamino-s-triazine	OCH_3	NHC_2H_5	NH_2
185	8.56	101,143,153	M-OOIT	2-Hydroxy-4-hydroxy-6-isopropylamino-s-triazine	OCH_3	OH	$NHCH(CH_3)_2$
198	8.95	127,198	M-OEET	2-Methoxy-4,6-diethylamino-s-triazine	OCH_3	NHC_2H_5	NHC_2H_5
212	9.56	170,212	M-OIET	2-Methoxy-4-isopropylamino-6-ethylamino-s-triazine	OCH_3	NHC_2H_5	$NHCH(CH_3)_2$
212	10.43	170,212	M-ODET	2-Methoxy-4-acetamindo-6-ethylamino-s-triazine	OCH_3	NHC_2H_5	$NHCOCH_3$
226	11.63	184,198,226	M-ODIT	2-Methoxy-4-acetamindo-6-isopropylamino-s-triazine	OCH_3	$NHCOCH_3$	$NHCH(CH_3)_2$
246(ESI)	20.28	196,204,246	M-COEIT	2-Chloro-4-(2-methoxy-ethylamino)-6-isopropylamino-s-triazine	Cl	$NHCH(OCH_3)CH_3$	$NHCH(CH_3)_2$

current was 5 μA and the sheath gas flow rate was 25AU (APCI) or 18AU (ESI).

3. Results and discussion

3.1. Photolytic degradation of atrazine

The reduction of atrazine as a function of irradiation time is depicted in Fig. 2. It was obviously seen from the figure that atrazine was photolyzed quickly in first 30 min and its corresponding removal is 70%. And then the degradation gradually slowed down, 90% atrazine was degraded in 50 min. The photodegradation of atrazine followed the first order kinetics [15] and its degradation rate constant was about 0.0411 min^{-1}. It is well known that atrazine could be decomposed into some acidic substances such as cyanuric acid, ammelide, and ammeline [11]. The variation of solution pH was also investigated in this study, and the result was presented in Fig. 1. It was easily observed that the pH of the solution decreased with the increase of irradiation time and varied from 5.8 to 4.98.

The UV–vis absorption spectra of the reaction solutions were recorded by a Shimadzu 123 UV-2450 spectrophotometer (Japan). The absorption wavelength of atrazine and its main intermediates ranged from 200 to 300 nm [16,17], in good agreement with previous report [18]. As shown in Fig. 3, there was a intense band around 220 nm and a rather weak one around 265 nm, the 220 nm band previously was assigned to a π to π* transition [19], the 265 nm was assigned to n to π* [20]. It was noted from the figure that good isosbestic points were observed, indicating clean interconversion to the primary products [18]. In the first 30 min, the absorption value at the maximum absorption wavelength of 220 nm decreased gradually, indicating that UV irradiation induced fast decomposition of atrazine. The slight blue shit was observed from Fig. 3, which may be caused by theoretically partial or complete loss of lateral chains and substitution amino by hydroxyl group. It was noted that the initial absorption bands disappeared after 50 min irradiation, there were two distinct absorptions at about 210 and 240 nm, respectively. The peak at 210 nm might be caused by formation of cyanuric acid, ammelide and ammeline [17]. The chromophoric group of heteroatom ring, such as –Cl, was possibly replaced by –OH, which led to larger conjugative effect.

3.2. Degradation products and mechanism

3.2.1. Identification of degradation products

In order to assess all the available photodegradation products, the samples with different degradation intervals (10, 30, 60, 90, 120 min) were collected to identify by LC–MS/MS technique. All the identified degradation products and their retention time, names, formulae, and structures are classifiedly presented in Table 1.

Major photodegradation products of atrazine containing seven classes are shown in Table 1. Class A resulted from dechlorination-hydroxylation reaction, prominently represented by OIET. Then dechlorinated product underwent a dealkylation process to produce the dechloro-dealkylated products (OAAT, OEAT, OIAT, OIMT, OEET, etc.), labeled as Class B. Class C was produced through direct dealkylation, including CMIT, CIAT, CEAT, etc. The products in Class D, such as OOET, OOIT etc, resulted from substitution amidogen by hydroxyl group. Besides, several compounds were found to contain an acetamide-aldehyde group, displayed as Class E, which resulted from oxidation of alkyl group in lateral chains. Class F was produced through dehydrogenation-olefination process, taking OOVT, OVET for example. In the present study, we identified a series of dechlorination-hydrogenated products (EIST, NEST, VEST, IAST, EAST, and OOST). In which, only EIST has been detected in microwave-assisted photocatalytic process [18], others were not reported previously. Mass spectra of some new products of atrazine including TIC for specific mass and ionic spectra for specific detected by LC–MS/MS were illustrated in Fig. 4.

Besides, a series of dechlorination-methoxylation products (Class H) were also detected in reaction solution, these products might be caused by slight amount of methanol from reserving liquid.

3.2.2. Variations of main products

HPLC chromatograms of the atrazine solutions at different irradiation intervals were recorded by a UV–vis diode array detector at 215 nm. Peak a (t_R = 8.34 min) was atrazine, and it was obviously seen that atrazine decreased quickly and was almost completely degraded in 50 min, presented in Fig. 5. For more distinct observation, the chromatograms at 10 and 50 min irradiation were

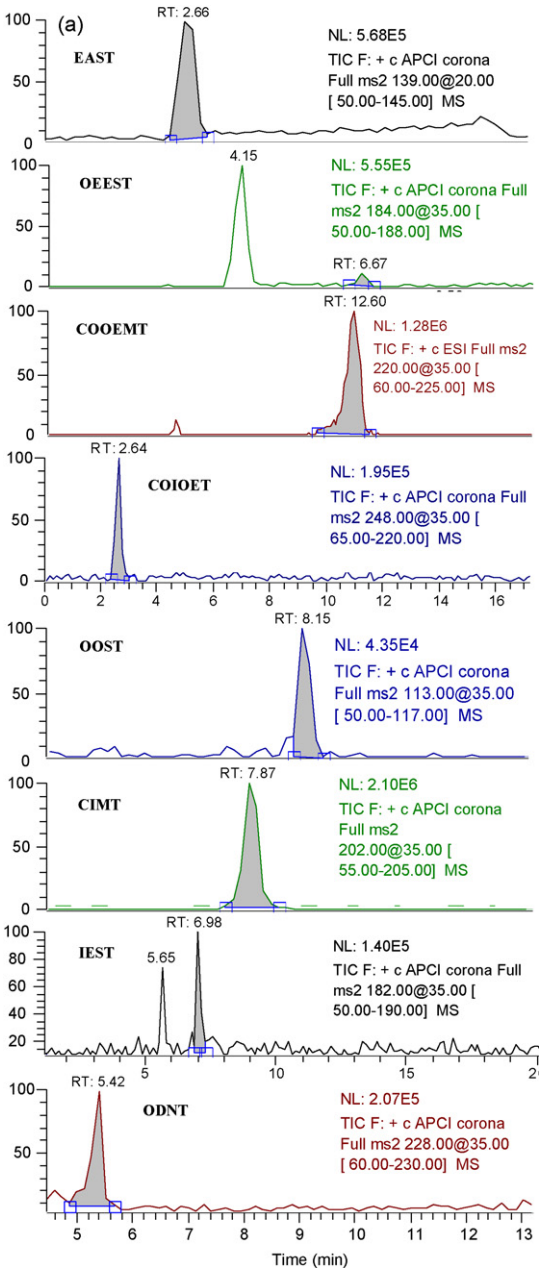

Fig. 4. Mass spectra (TIC for specific mass and ionic spectra for specific) of some new products from direct photolytic degradation process detected by LC–MS\MS.

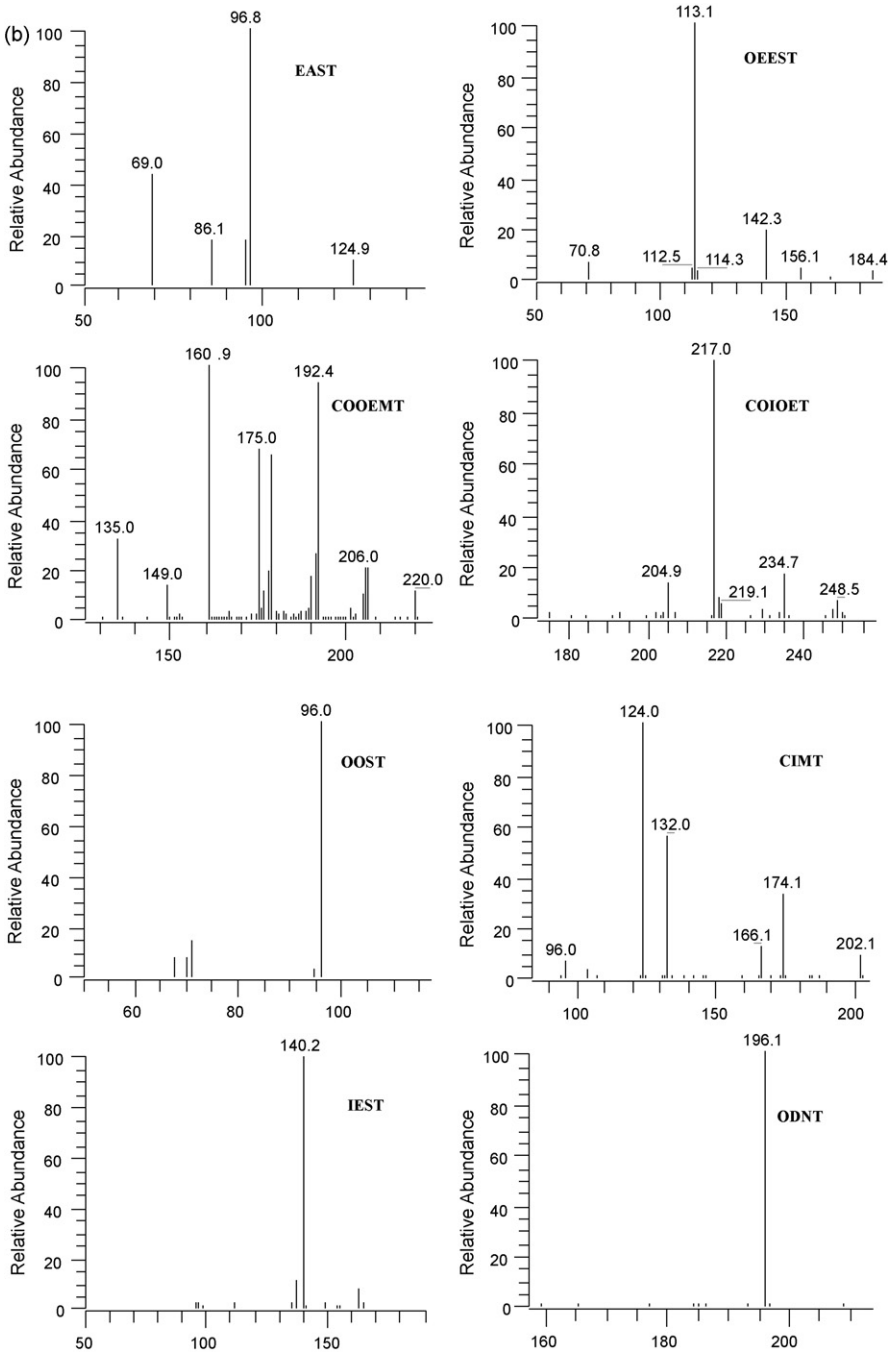

Fig. 4. (*Continued*).

enlarged. The Peaks of b, c, d, f, e, g, h and i were M-OIET, M-OEET, CVVT, CIMT, CEAT, OIET, OIMT, and ODET, respectively. And Peak j might be impurity in the solvent. It was obviously observed that the concentration of dechlorination-hydroxylation product OIET was the largest among all degradation products, which was in agreement with the previous report [2,9]. It was noted that CIMT (Peak e) was one of the major products at 10 min, but it was decomposed soon and almost disappeared during 50 min. Whereas, other degradation products were formed and reached gradually the maximum at 50 min, and then they also began to degrade slightly. The exact changes of peak areas of atrazine and its main degradation products recorded as a function of irradiation time were more clearly displayed in Fig. 6.

3.2.3. Possible degradation mechanism

Based on the degradation products described above, possible degradation pathways were proposed in Fig. 7.

It was well documented that UV radiation would result in the decomposition of organic molecules by bond cleavage and free radical generated [21]. Our calculation results (presented in Table 2) indicated that the bond length of C–Cl bond (1.734 Å) was the longest among all bonds and the bond polarity (0.293) was relatively lower, so it was the easiest to be scissile compared with any other bonds. These were well consistent with the experiment result, in which dechlorination occurred easily and promptly. The dechlorination maybe result either from a homolytic cleavage of the C–Cl bond or the heterolytic cleavage of the excited

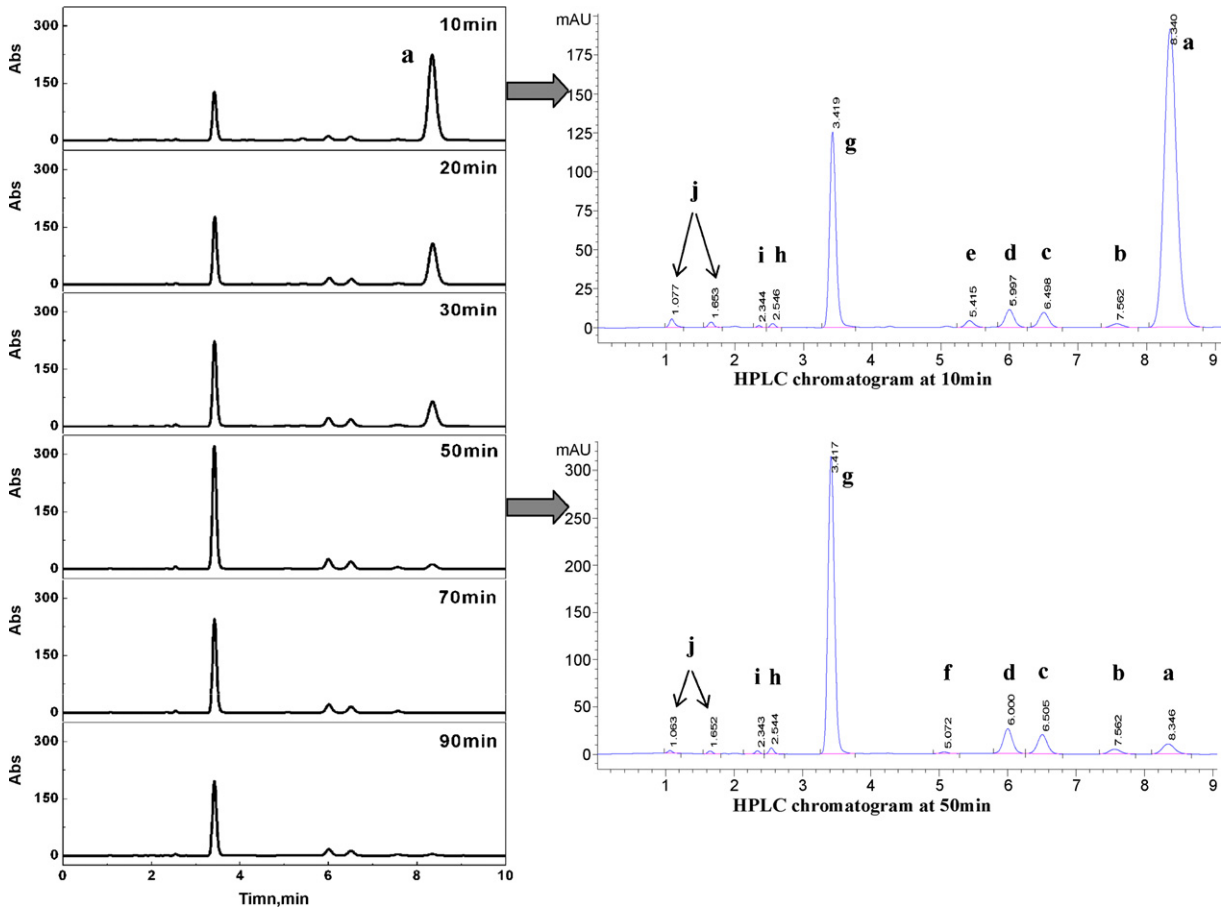

Fig. 5. HPLC chromatograms of atrazine and its main products at different irradiation intervals.

state atrazine molecule in polar solvents such as water [10]. Most documents mentioned that the first step of the degradation mechanism consisted of fast dechlorination-hydroxylation (Path 2 in Fig. 7a), and it formed the maximum product OIET which appeared to be quite stable in direct photolysis and to undergo dealkylation at a very low rate. However, not all dechlorinated products completely transformed into OIET. The dechloro-hydrogenated products meaned the presence of another dechlorination way in our studies, illustrated in Path 4, Fig. 7b, which were never reported in direct photolysis of atrazine. It might be attributed to the fact that atrazine absorbed the 254 nm UV light to cause the C–Cl bond directly cleave under the intense UV radiation [21]. It was noted that this result may be from a minor process since compounds containing such a structure were found as traces.

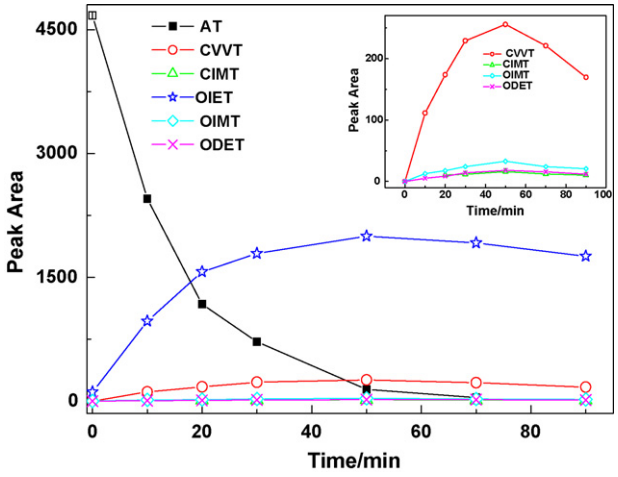

Fig. 6. Changes of peak areas of atrazine and its main degradation products vs irradiation time (the unclear parts of the figure have been enlarged and is shown in inset).

Besides, C–N bond and C–C bond in amino-alky groups such as N(8)–C(10), N(11)–C(12), C(9)–C(10), C(12)–C(13), C(12)–C(14) might also cleave easily and induced dealkylation process. Chloro-dealkylation and dechloro-dealkylation processes were marked as Path 1 and Path 4 in Fig. 7a, respectively. The bond polarity of C–C (0.343) in ethylamino group was somewhat smaller than that in isopropylamino group (0.366 and 0.365), inferring that deethylation should be easier than deisopropylation, which was supported by the detection of CIMT and relatively larger amount of CEAT than CIAT, and confirmed the previous work [17]. Torrents et al. [11] thought that the chloro-dealkylated products such as CEAT and CIAT, were the principle products of ·OH systems, and no dechloro-dealkylated products were found under the irradiation of UV wavelength beyond 290 nm. However, a number of dechloro-dealkylated (i.e. OIMT, OEAT, OIAT) appeared under the 254 nm UV irradiation in our experiments, which was in accordance with the study reported by Claudia et al. [9]. So it was considered that the dealkylation followed dechlorination might be caused by the bond rupture under shorter wavelength irradiation because of the longer bond length of C–C and lower bond polarity of N–C in amino-alky groups (shown in Table 2).

During photolysis, the excited organics could transfer the energy directly to the substrate (sensitization), undergo electron transfer with the substrate, or cause a series of reactions with the subsequent formation of oxidants such as hydroxy radical [11]. When dealkylation was completed and only amino group remained on the lateral chain of heterocycle, C(2) and C(4) might be attacked by the hydroxyl radicals owing to their high Mulliken atomic charges and the decrease in steric hindrance, and then deamination-hydroxylation process occurred, which resulted in substituting amino group by hydroxyl group, shown in Path 6, Fig. 7a. Ta et al. [2] pointed out that only after the dealkylation, the deamination-hydroxylation was likely to occur.

Alkylic-oxidation process (Path 3 in Fig. 7a) was proved by the identification of CDIT, CDDT, ODIT, ODET etc. In ethylamino group,

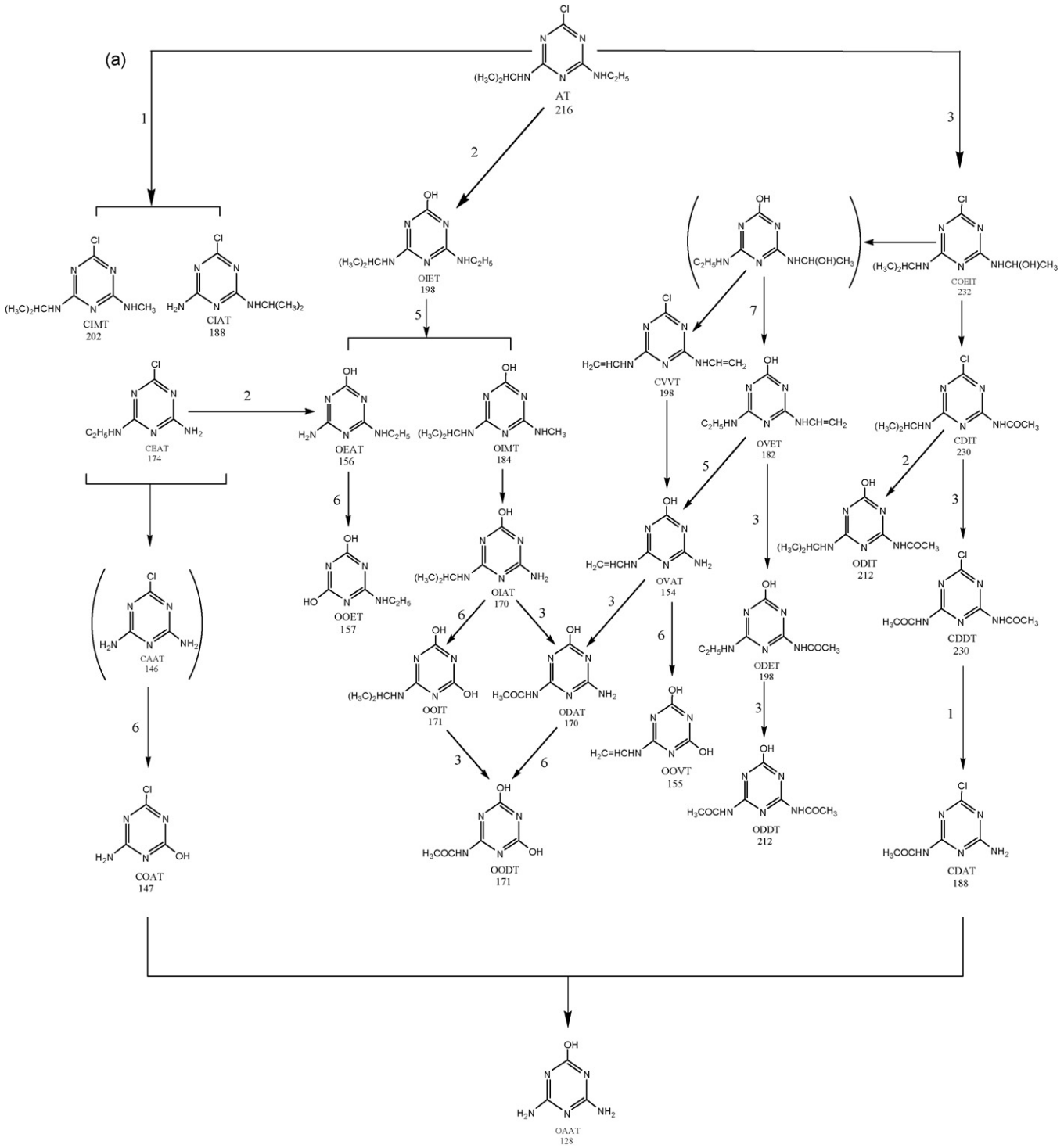

Fig. 7. Direct degradation mechanism of atrazine: (1) chloro-dealkylation, (2) dechlorination-hydroxylation, (3) alkylic-oxidation, (4) dechlorination-hydrogenation, (5) dechloro-dealkylation, (6) deamination-hydroxylation, (7) olefination (the products inside brackets were not detected in our experiments, but were observed by other groups, or postulated.).

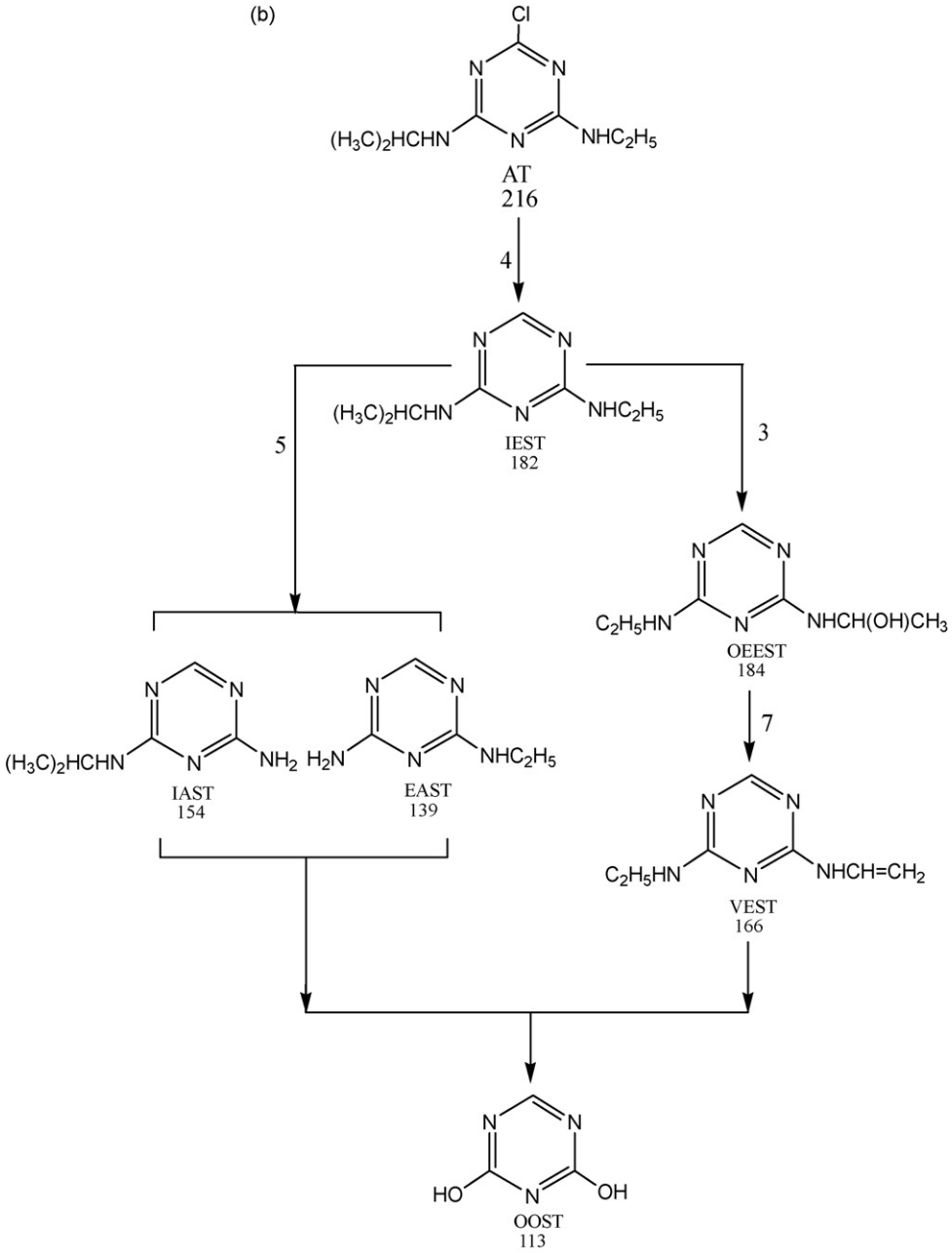

Fig. 7. (*Continued*).

possible reaction course followed:

$$RNH - CH_2 - CH_3 \xrightarrow{^{\bullet}OH} RNH - CHOH - CH_3 \quad (1)$$

$$RNH - CHOH - CH_3 \xrightarrow{^{\bullet}OH} RNH - COCH_3 \quad (2)$$

while in the case of the isopropylamino group, the alkylic-oxidated products might be produced in parallel but through a different sequence [22]:

$$RNH - CH(CH_3)_2 \xrightarrow{^{\bullet}OH} RNH - C(CH_3)_2 - OH \quad (3)$$

$$RNH - C(CH_3)_2 - OH \xrightarrow{-H_2O} RN = C(CH_3)_2 \rightleftharpoons RNH - C(CH_3) = CH_2 \quad (4)$$

$$RNH - C(CH_3) = CH_2 \xrightarrow{^{\bullet}OH} RNH - COCH_3 \quad (5)$$

Olefination leading to the vinylamine form was observed in the present study (Path 7 in Fig. 7a). This also resulted in an attack of hydroxy radical and dehydration process [22]:

$$RNH - CH_2 - CH_3 \xrightarrow{^{\bullet}OH} RNH - CHOH - CH_3 \quad (6)$$

$$RNH - CHOH - CH_3 \xrightarrow{-H_2O} RNH - RN = CH - CH_3 \rightleftharpoons RNH - CH = CH_2 \quad (7)$$

Besides, olefinic products could be further oxidized to form carbonylamino group [2].

To all appearances, OAAT and OOST was the final degradation products of atrazine in our given conditions, and no trace of OOAT or OOOT could be detected. But they ought to be eventually formed when a sufficient intensity of irradiation is provided with an extended time [2].

Table 2
Mulliken atomic charges, bond length and polarity of atrazine calculated by Gaussian 03, the theoretical model, denoted B3LYP, is based on density functional theory, and the 6-31G(d,p) basis set was used

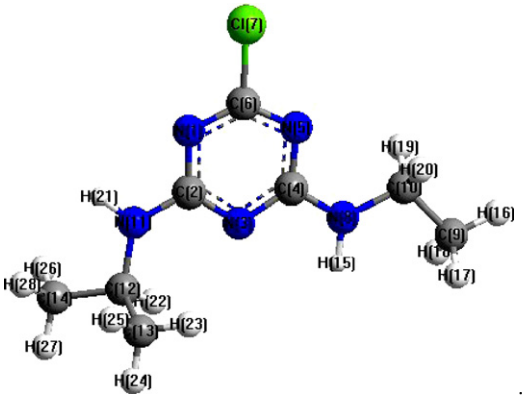

Element	Mulliken atomic charges	Bond	Bond Length (A^0)	Bond	Bond Polarity
N(1)	−0.625	N(1)–C(2)	1.347	N(1)–C(2)	0.496
C(2)	0.895	N(3)–C(2)	1.320	N(3)–C(2)	0.482
N(3)	−0.715	N(3)–C(4)	1.330	N(3)–C(4)	0.503
C(4)	0.898	N(5)–C(4)	1.336	N(5)–C(4)	0.483
N(5)	−0.633	C(6)–N(1)	1.298	C(6)–N(1)	0.465
C(6)	0.395	N(5)–C(6)	1.308	N(5)–C(6)	0.451
Cl(7)	0.038	C(6)–Cl(7)	1.734	C(6)–Cl(7)	0.293
N(8)	−0.840	C(4)–N(8)	1.333	C(4)–N(8)	0.358
C(9)	−0.522	N(8)–C(10)	1.453	N(8)–C(10)	0.196
C(10)	−0.066	C(9)–C(10)	1.522	C(9)–C(10)	0.343
N(11)	−0.835	N(11)–C(2)	1.335	N(11)–C(2)	0.360
C(12)	0.057	N(11)–C(12)	1.457	N(11)–C(12)	0.199
C(13)	−0.474	C(12)–C(13)	1.529	C(12)–C(13)	0.366
C(14)	−0.494	C(12)–C(14)	1.526	C(12)–C(14)	0.366
H(15)	0.398	H(15)–N(8)	0.994	H(15)–N(8)	0.323
H(16)	0.183	H(16)–C(9)	1.084	H(16)–C(9)	0.397
H(17)	0.170	H(17)–C(9)	1.086	H(17)–C(9)	0.388
H(18)	0.171	H(18)–C(9)	1.086	H(18)–C(9)	0.388
H(19)	0.190	H(19)–C(10)	1.083	H(19)–C(10)	0.415
H(20)	0.189	H(20)–C(10)	1.083	H(20)–C(10)	0.415
H(21)	0.400	N(11)–H(21)	0.996	N(11)–H(21)	0.320
H(22)	0.206	C(12)–H(22)	1.081	C(12)–H(22)	0.423
H(23)	0.186	H(23)–C(13)	1.083	H(23)–C(13)	0.393
H(24)	0.158	H(24)–C(13)	1.086	H(24)–C(13)	0.384
H(25)	0.157	H(25)–C(13)	1.086	H(25)–C(13)	0.385
H(26)	0.181	H(26)–C(14)	1.084	H(26)–C(14)	0.392
H(27)	0.174	C(14)–H(27)	1.085	C(14)–H(27)	0.394
H(28)	0.159	C(14)–H(28)	1.087	C(14)–H(28)	0.385

4. Conclusions

Atrazine in aqueous solutions could be rapidly decomposed under 254 nm UV irradiation in given reaction time and its corresponding reaction kinetic constant was about 0.0411 min^{-1}. Based on HPLC and HPLC–MS/MS technique, numerous intermediates were separated and identified. The phototransformation of atrazine almost occurred at C–Cl bond and amino-alky group, rather than opened the heteroatom ring. Direct photolysis mainly proceeded through the following seven pathways: chloro-dealkylation, dechlorination-hydroxylation, alkylic-oxidation, dechlorination-hydrogenation, dechloro-dealkylation, deamination-hydroxylation and olefination, in which, dechlorination-hydrogenation was a new reaction as to photolytic degradation of atrazine never mentioned previously.

Acknowledgements

The authors greatly acknowledge the National Major Project of Science & Technology Ministry of China (Grant no. 2008ZX07421-002 and 2008ZX08526-003) and National Supporting Project of Science & Technology Ministry of China (2006BAJ08B06) for financial support.

References

[1] M. Graymore, F. Stagnitti, G. Allinson, Impacts of atrazine in aquatic ecosystems, Environ. Int. 26 (2001) 483–495.
[2] N. Ta, J. Hong, T.F. Liu, C. Sun, Degradation of atrazine by microwave-assisted electrodeless discharge mercury lamp in aqueous solution, J. Hazard. Mater. 138 (2006) 187–194.
[3] G. Cimino-Reale, D. Ferrario, B. Casati, R. Brustio, C. Diodovich, A. Collotta, M. Vahter, L. Gribaldo, Combined in-utero and juvenile exposure of mice to arsenate and atrazine in drinking water modulates gene expression and clonogenicity of myeloid progenitors, Toxicol. Lett. 180 (2007) 59–66.
[4] T.B. Hayes, S. Collins, M. Lee, M. Mendoza, N. Noriega, A.A. Stuart, A. Vonk, Hermaphroditic, demasculinized frogs after exposure to the herbicide atrazine at low ecologically relevant doses, Proc. Natl. Acad. Sci. U.S.A. 99 (2002) 5476–5480.
[5] T. Hayes, K. Hasten, M. Tsui, A. Hoang, C. Haeffele, A. Vonk, Atrazine-induced hermaphroditism at 0.1 ppb in American leopard frogs, Environ. Health Perspect. 111 (2003) 568–575.

[6] R.L. Cooper, T.E. Stoker, J.M. Goldman, M.B. Parrish, L. Tyrey, Effect of atrazine on ovarian function in the rat, Reprod. Toxicol. 10 (1996) 257–264.
[7] S.H. Swan, R.L. Kruse, F. Liu, D.B. Barr, E.Z. Drobnis, J.B. Redmon, C. Wang, C. Brazil, J.W. Overstreet, Semen quality in relation to biomarkers of pesticide exposure, Environ. Health Perspect. 111 (2003) 1478–1484.
[8] R.N. Lerch, W.W. Donald, Y.X. Li, Hydroxylated atrazine degradation products in a small Missuri stream, Environ. Sci. Technol. 29 (1995) 2759–2768.
[9] L.B. Claudia, P. Carlo, R. Vittorio, S. Elena, Mechanism and efficiency of atrazine degradation under combined oxidation processes, Appl. Catal. B: Environ. 64 (2006) 131–138.
[10] V. Hequet, C. Gonzalez, P. Le, Cloirec photochemical processes for atrazine degradation: methodological approach, Water Res. 35 (2001) 4253–4260.
[11] A. Torrents, B.G. Anderson, S. Bilboulian, W.E. Johnson, C.J. Hapeman, Atrazine photolysis: mechanistic investigations of direct and nitrate-mediated hydroxy radical processes and the influence of dissolved organic carbon from the chesapeake bay, Environ. Sci. Technol. 31 (1997) 1476–1482.
[12] E. Pellzzetti, V. Maurlno, C. Minero, Photocatalytic degradation of atrazine and other s-triazine herbicides, Environ. Sci. Technol. 24 (1990) 1559–1565.
[13] F.J. Beltran, M. Gonzalez, F.J. Rivas, P. Alvarez, Aqueous UV radizion and UV/H_2O_2 oxidation of atrazine first degradation products: deethylatrazine and deisopropylatrazine, Environ. Toxicol. Chem. 15 (1996) 868–872.
[14] A. Hiskia, M. Ecke, A. Troupis, A. Kokorakis, H. Hennif, E. Papaconstantinou, Sonolytic, photolytic, and photocatalytic decomposition of atrazine in the presence of polyoxometalates, Environ. Sci. Technol. 35 (2001) 2358–2364.
[15] J. Arantegui, J. Prado, E. Chamarro, Kinetics of the UV degradation of atrazine in aqueous solution in the presence of hydrogen peroxide, J. Photochem. Photobiol. A: Chem. 88 (1995) 65–74.
[16] K.H. Chan, W. Chu, Model applications and intermediates quantification of atrazine degradation by UV-enhanced fenton process, J Agric. Food Chem. 54 (2006) 1804–1813.
[17] E.B. Marianne, B. Sulzberger, Atrazine degradation in irradiated iron/oxalate systems: effects of pH and oxalate, Environ. Sci. Technol. 33 (1999) 2418–2424.
[18] M.E.D.G. Azenha, H.D. Burrows, M. Canle, et al., Kinetic and mechanistic aspects of the direct photodegraclation of atrazine, atraton, ametryn and 2-hydroxyatrazine by 254 nm light in aqueous solution, J. Phys. Org. Chem. 16 (2003) 498–503.
[19] B.E. Pape, M.F. Para, M.J. Zabik, Photochemistry of bioactive compounds-photodecomposition of 2-(1,3-dioxolane-2-yl)-phenyl-*n*-methyl carbamate, J. Agric. Food Chem. 18 (1970) 490–493.
[20] S.F. Mason, The electronic spectra of *N*-heteroaromatic systems. Part I. The $n \rightarrow \pi$ transitions of monocyclic azines, J. Chem. Soc. (1959) 1240–1246.
[21] Z.Q. Gao, S.G. Yang, N. Ta, C. Sun, Microwave assisted rapid and complete degradation of atrazine using TiO_2 nanotube photocatalyst suspensions, J. Hazard. Mater. 145 (2007) 424–430.
[22] S. Nealieu, L. Kerhoas, J. Einhorn, Degradation of atrazine into ammeline by combined ozone/hydrogen peroxide treatment in water, Environ. Sci. Technol. 34 (2000) 430–437.